



DE GRUYTER  
OPEN

# ARCHIVES OF MECHANICAL TECHNOLOGY AND MATERIALS

WWW.AMTM.PUT.POZNAN.PL



## Identifying Combination of Friction Stir Welding Parameters to Maximize Strength of Lap Joints of AA2014-T6 Aluminum Alloy

C. Rajendran<sup>a\*</sup>, K. Srinivasan<sup>a</sup>, V. Balasubramanian<sup>a</sup>, H. Balaji<sup>b</sup>, P. Selvaraj<sup>b</sup>

<sup>a</sup> Centre for Materials Joining and Research (CEMAJOR), Department of Manufacturing Engineering, Annamalai University, Annamalaiagar-608002

<sup>b</sup> Aeronautical Development Agency (ADA), Bangalore  
e-mail address: crdrn12@yahoo.com

### ARTICLE INFO

Received 23 December 2016  
Received in revised form 09 February 2017  
Accepted 13 February 2017

### KEY WORDS

Friction stir welding,  
Aluminum alloy,  
Response surface methodology,  
Lap joint,  
Tensile strength

### ABSTRACT

AA2014 aluminum alloy (Al-Cu alloy) has been widely utilized in fabrication of lightweight structures like aircraft structures, demanding high strength to weight ratio and good corrosion resistance. The fusion welding of these alloys will lead to solidification problems such as hot cracking. Friction stir welding is a new solid state welding process, in which the material being welded does not melt and recast. Lot of research works have been carried out by many researchers to optimize process parameters and establish empirical relationships to predict tensile strength of friction stir welded butt joints of aluminum alloys. However, very few investigations have been carried out on friction stir welded lap joints of aluminum alloys. Hence, in this investigation, an attempt has been made to optimize friction stir lap welding (FSLW) parameters to attain maximum tensile strength using statistical tools such as design of experiment (DoE), analysis of variance (ANOVA), response graph and contour plots. By this method, it is found that maximum tensile shear fracture load of 12.76 kN can be achieved if a joint is made using tool rotational speed of 900 rpm, welding speed of 110 mm/min, tool shoulder diameter of 12 mm and tool tilt angle of 1.5°.

### 1. INTRODUCTION

High strength, aluminum alloys (Al) are widely used in aircraft and automobile industries. It is very difficult to join these alloys by fusion welding processes, as it results in solidification problems like hot cracking, alloy segregation, grain coarsening etc. Friction stir welding (FSW) is a solid state welding process, invented by The Welding Institute (TWI) UK and patented in 1991 [1]. This opened up new area in materials joining. Using FSW, high productivity and high quality welds of aluminum 2xxx and 7xxx series alloys, are now possible. Initially, this process was principally applied for making butt joints in Al alloys, now use of FSW in lap joint

configuration would expand the applications in aircraft structures. The FSW of lap joints may substitute other joining processes like spot welding, riveting, soldering and brazing on the ground of full intensity. In lap joint, the tool pin must only reach to the bottom of the sheet and create a metallurgical bonding between the two sheets.

Riveting is the primary joining method in all the aircraft structures involving aluminum alloys, since, 1920 [2]. The maximum shear strength obtained was 10.3 kN using aluminum alloy solid rivets [single rivet] 9.2 kN using blind fasteners, and 14.4 kN using Ti-6Al-4V swaged collar fasteners [3]. Firouz et al [4] investigated the effect of rotational speed on microstructural characteristics of friction

stir lap welded (FSLW) AA6061-T6 aluminum alloy, and found that the hardness distribution of joint was closer to base metal in the upper and lower sheet, when the tool rotational speed was lower. Urso et al [5] reported the influence of process parameters and tool geometry on mechanical properties of FSLW joints of aluminum alloys, using two different types of tools with and without threads. It was found that the use of threaded pin leads to improvement in mechanical and metallurgical properties. Yazdanion et al [6] analyzed the effect of FSLW parameters on joint strength of AA6060 and found that the tool rotational speed and pin length are the major influencing parameters to obtain the sound joints.

Sundrarajan et al [7] investigated the effect of tool rotational speed, welding speed and plunge depth on FSLW joints of AA5182 and AA6022 dissimilar aluminum alloys. The failure location was found in the advancing side, as it had experienced high temperature gradient than the retreating side during welding. Kimapong et al [8] investigated the effect of process parameters on mechanical properties of FSLW joint between aluminum and steel. The shear strength couldn't be increased with increase of tool tilt angle and tool diameter due to formation of intermetallic at the joint interface. Cen et al [9] investigated the material flow joint structure and strength of FSLW joints of Al-to-Al and Mg-to-Mg. It was found that hook continuity and hooking direction was highly influenced by the welding conditions. Babu et al [10] analyzed the effect of temper conditions (T4 & T6) and alclad layer on microstructural and mechanical properties of FSLW joints of AA2014 aluminum alloy. It was found that shear strength does not vary with change in temper conditions and also the presence of alclad layer.

Galvao et al [11] attempted to join two different types of aluminum alloys (heat treatable and non-heat treatable aluminum alloy) with copper by FSLW process, and reported low material mixing between AA5083 (non heat-treatable) with copper and uniform material mixing between AA6012(heat-treatable) with copper. Buffa et al [12] investigated the effect of process parameters on the mechanical and metallurgical properties of FSLW joints of AA2198-T4 by varying the joint configuration, tool rotational speed and tool geometry. It was found that the cylindrical conical pin and correct sheet positioning increased the weld nugget extension and improved the mechanical properties of the joint. Chen et al [13] used micro X ray method to analyze phase transition in the FSLW joints of aluminum and magnesium alloys, and found a conversion zone between stir zone and lower sheet metal. This zone contained intermetallic compounds Al<sub>12</sub> Mg<sub>13</sub>, Al<sub>3</sub> Mg<sub>2</sub>, and Mg<sub>2</sub> Si at lower welding speed and resulted in defects free region and improved the joint strength.

Salari et al [14] investigated the effect of FSLW parameters on microstructural characteristics and mechanical properties of AA5456 aluminum alloy plates with various thickness and temper conditions. Using four different types of pin tools (conical threaded, cylindrical-conical threaded, stepped conical thread pin, and flared triflute pin), it was found that stepped conical thread pin produced homogeneous microstructure with finer grains than other tools. However, the effect of tool rotational speed and welding speed on the macrostructure and defect formation in FSLW

joints of AA5456 aluminum alloy is that lower welding speed produced less hook height and higher welding speed produced kissing bond defect. While increased the tool rotational speed results in increasing hooking region [15]. Zhengwei et al [16] analyzed the effect of external stationary shoulder on joint appearance and lap shear strength of FSLW alclad 2024 aluminum alloy. Stationary shoulder was found to be more beneficial to the joint formation and avoids arc corrugation, flash and voids.

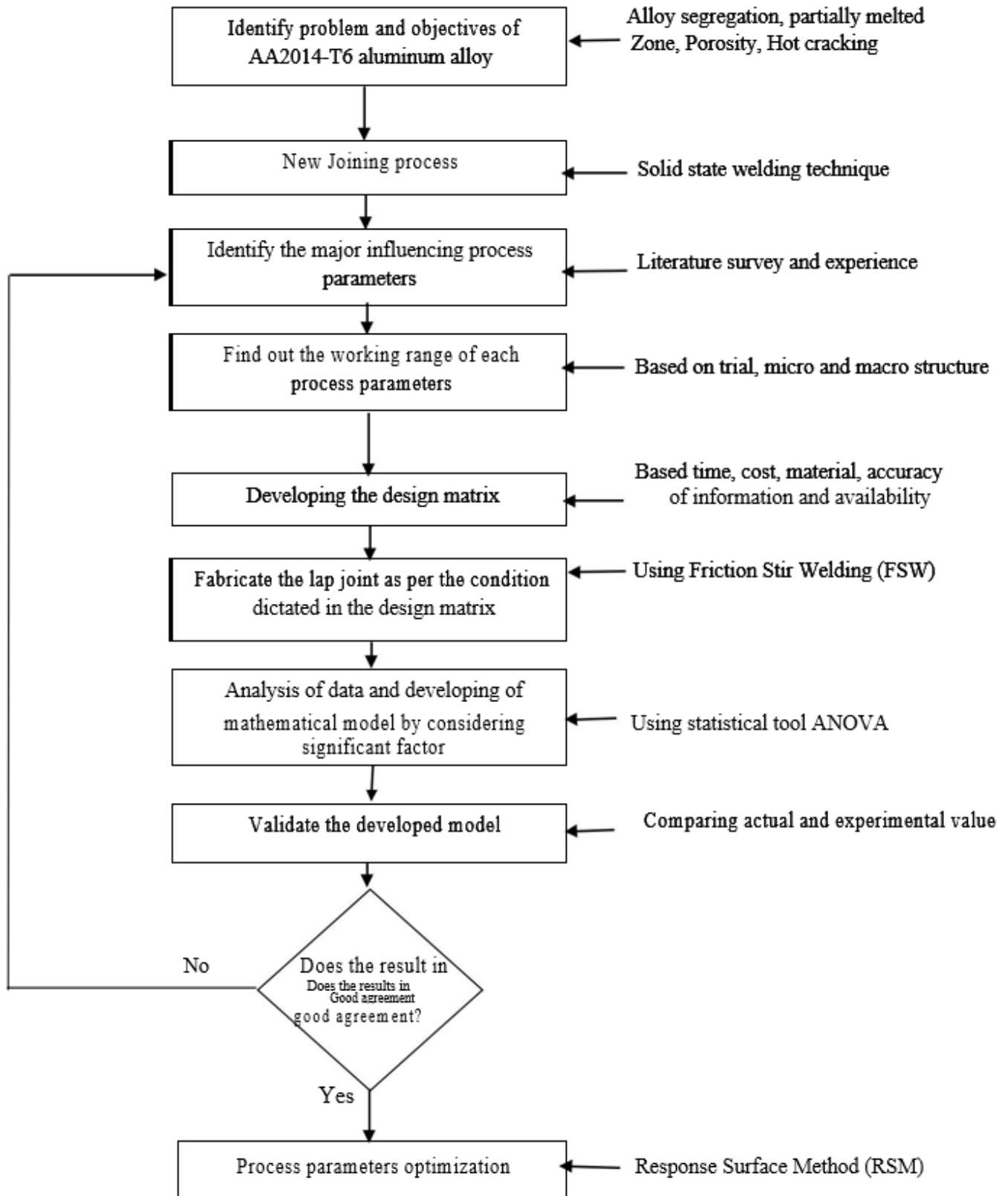
From the literature review [3-16], it is understood that the FSW parameters play major role in deciding the quality of the joints. Though lot of research works have been carried out to understand the effect of FSLW parameters individually on mechanical properties and microstructural characteristics, no attempt has been made so far to study the combined effect of all the parameters in a scientific method. Hence, in this investigation, an attempt has been made to optimize the few important FSW parameters to achieve maximum tensile strength in friction stir lap welded AA2014-T6 aluminum alloy joints by response surface methodology (RSM).

## 2. EXPERIMENTAL

The rolled sheets of AA2014-T6 aluminum alloy of 2 mm thick were used as the base metal in this investigation. The nominal chemical composition and mechanical properties of the base metal are given in Table 1 and Table 2, respectively. The optimization procedure used in this investigation is shown in Figure 1. Figure 2 shows joint configuration to fabricate the joints. The base metal is highly composed of elongated grains with uneven distribution of second phase particles (Fig. 3). The average grain size of the base metal is 30µm. The non-consumable tool made of super HSS (Fig. 4 and Fig. 5), with threaded taper pin profile and concave shoulder of 0.80 was used to fabricate the joints. The dimension of the tool used is presented in Table 3. A computer numerical controlled friction stir welding machine was used to fabricate the lap joints. Large numbers of trial experiments were conducted to determine the feasible working range of the FSLW parameters (Table 4), by varying any one of the process parameters and keeping the rest of them at a constant value. Table 5 shows the important factors and their levels. For the purpose of minimizing the experimental work, design of experiments (DoE) was applied. Four factors, five level central composite rotatable design matrix was selected to minimize experimental conditions. The design matrix (Table 6) consists of 30 set of coded conditions and comprising a full replication four factor factorial designs of 16 points, eight star points and six center points. The upper and lower limits of each parameter are coded as +2 and -2 respectively, and other three are equal intervals of upper and lower values. The coded values for intermediate levels can be calculated using the equation.

$$X_i = 2X - (X_{\max} + X_{\min}) / (X_{\max} - X_{\min}) \quad (1)$$

where, X is the required coded value of a variable from  $X_{\min}$  to  $X_{\max}$ .



*Fig.1. Flow chart for process optimization*

*Table 1. Chemical composition (wt. %) of base metal*

Si	Fe	Cu	Mn	Mg	Zn	Cr	Ti	Al
0.874	0.135	4.815	0.813	0.734	0.063	0.005	0.011	92.45

*Table 2. Mechanical properties of base metal*

Material	Yield stress (MPa)	Ultimate tensile stress (MPa)	Elongation (%)	Micro hardness 50g, 15 sec (HV)	Shear load (kN)
AA2014-T6	431	455	10	163	17

*Table 3. Dimensions of the tool used*

Pin description	Pin diameter		Pin length (mm)	Taper angle in pin diameter (°)	Thread pitch (mm)
	Major diameter (mm)	Minor diameter (mm)			
Threaded taper pin	6.0	5.0	5.75	4.96	0.75

Table 4. Macrostructure analysis for fixing the working range of FSLW



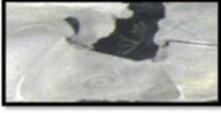

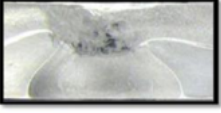


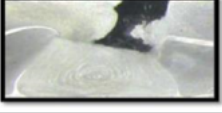
Parameters	Range	Macrograph	Name of the defect	Reason for defect
Tool rotational speed(N)	$N > 1100$ rpm		Cluster of worm hole	Excess heat input due to high heat input.
Tool rotational speed (N)	$N < 700$ rpm		Lack of fill	Insufficient heat input causes less plastic material flow
Welding speed (S)	$S > 130$ mm/min		Tunnel defect	Low plasticized material transportation
Welding speed (S)	$S < 90$ mm/min		Warm hole	High heat input
Tool shoulder diameter (D)	$D > 16$ mm		Cluster of worm holes	Excess heat input due to large area of contact
Tool shoulder diameter(D)	$D < 8$ mm		Tunnel defect	Low heat generation produced insufficient plasticized material transportation
Tool tilt angle (Q)	$Q > 3^\circ$		Cluster of warm hole	High forging pressure produced more strain hardening
Tool tilt angle(Q)	$Q < 1^\circ$		Lack of fill	Insufficient forging force resulted low plasticized material flow and consolidation

Table 5. Important factors and their levels

No	Parameters	Unit	Notation	Levels				
				-2	-1	0	+1	+2
1	Tool rotational speed	rpm	N	700	800	900	1000	1100
2.	Welding speed	mm/min	S	90	100	110	120	130
3	Tool shoulder diameter	mm	D	8	10	12	14	16
4	Tool tilt angle	°	Q	1.0	1.5	2.0	2.5	3.0

Table 6. Design matrix and experimental results

Exp. No	Coded value of welding parameters				Actual value of welding parameters				TSFL (kN)
	N	S	D	Q	N	S	D	Q	
1	-1	-1	-1	-1	800	100	10	1	8.28
2	+1	-1	-1	-1	1000	100	10	1	8.82
3	-1	+1	-1	-1	800	120	10	1	9.02
4	+1	+1	-1	-1	1000	120	10	1	10.1
5	-1	-1	+1	-1	800	100	14	1	9.53
6	+1	-1	+1	-1	1000	100	14	1	9.69
7	-1	+1	+1	-1	800	120	14	1	10.03
8	+1	+1	+1	-1	1000	120	14	1	10.74
9	-1	-1	-1	+1	800	100	10	2	9.09
10	+1	-1	-1	+1	1000	100	10	2	9.74
11	-1	+1	-1	+1	800	120	10	2	9.78
12	+1	+1	-1	+1	1000	120	10	2	10.1
13	-1	-1	+1	+1	800	100	14	2	10.23
14	+1	-1	+1	+1	1000	100	14	2	11.12
15	-1	+1	+1	+1	800	120	14	2	10.87
16	+1	+1	+1	+1	1000	120	14	2	10.9
17	-2	0	0	0	700	110	12	1.5	8.01
18	+2	0	0	0	1100	110	12	1.5	9.16
19	0	-2	0	0	900	90	12	0.5	9.11
20	0	+2	-2	0	900	130	12	2.5	11.03
21	0	0	+2	0	900	110	8	1.5	10.97
22	0	0	0	-2	900	110	16	1.5	12.8
23	0	0	0	+2	900	110	12	1.5	7.68
24	0	0	0	0	900	110	12	1.5	8.95
25	0	0	0	0	900	110	12	1.5	12.76
26	0	0	0	0	900	110	12	1.5	11.94
27	0	0	0	0	900	110	12	1.5	12.01
28	0	0	0	0	900	110	12	1.5	11.86
29	0	0	0	0	900	110	12	1.5	12.13
30	0	0	0	0	900	110	12	1.5	12.38

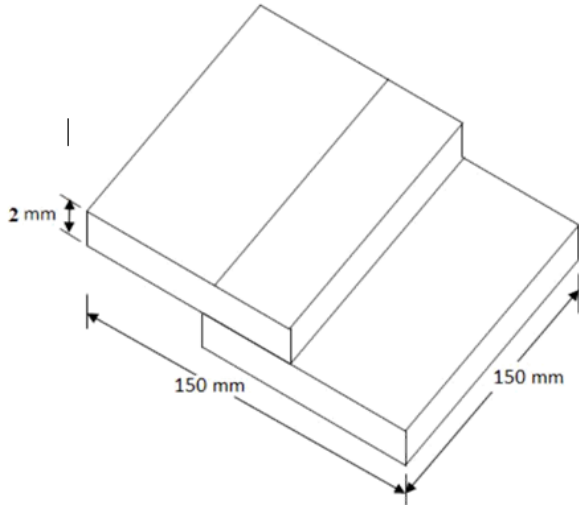


Fig. 2. FSLW joint configuration

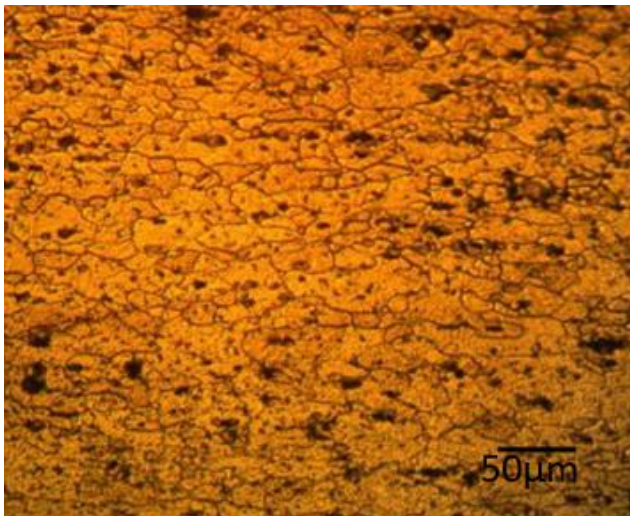


Fig. 3. Optical micrograph of base metal

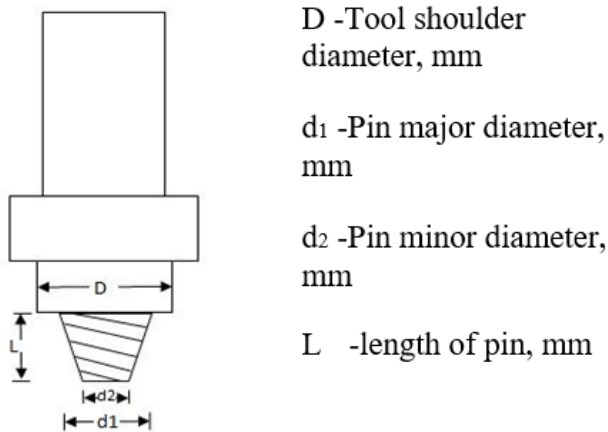


Fig. 4. Schematic diagram of FSLW tool

The lap joints were made as per the conditions dictated by the design matrix at random order so as to avoid systematic error creeping the results. Few of the fabricated lap joints are displayed in Fig. 6. The tensile specimens were extracted from the joints as per the AWS-SAE-D8.9.1 and shown in Fig. 7. The tensile shear fracture loads (TSFL) of the joints were evaluated using a 100 kN electromechanical controlled universal testing machine (make FIE-Blue Star, India model: UNITECK-94100). The specimen was loaded at the rate of 1.5 kN/min until the faying surfaces of specimens were sheared off, and the values were recorded. Three specimens were tested from each joint and the average was calculated and presented in Table 6.



Fig. 5. Fabricated FSW tools

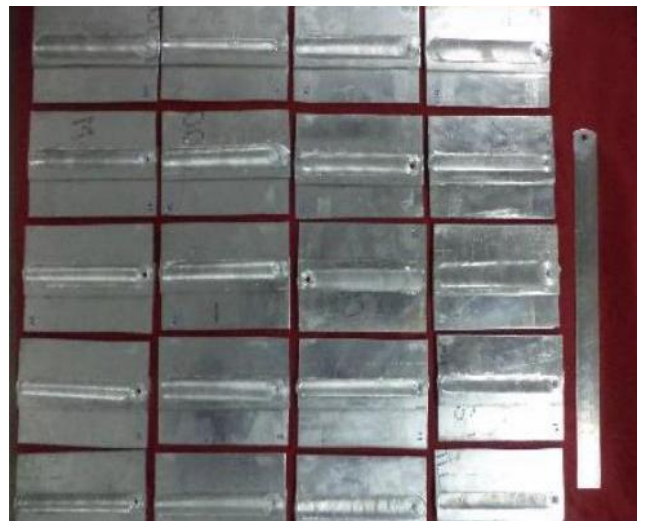


Fig. 6. Fabricated FSLW joints

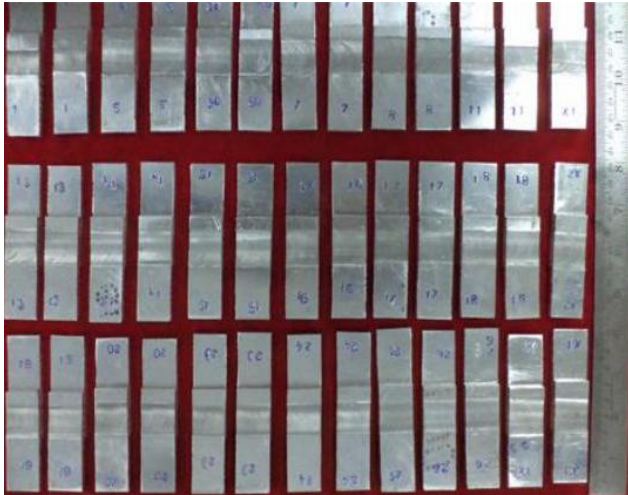


Fig. 7. Fabricated lap shear specimen

### 3. DEVELOPING AN EMPIRICAL RELATIONSHIP

Tensile shear fracture load (TSFL) of friction stir lap welded AA2014-T6 aluminum alloy is a function of the welding parameters such as tool rotation speed, welding speed, tool shoulder diameter, and tool tilt angle, and it can be expressed as

$$\text{TSFL} = f(N, S, D, Q) \quad (2)$$

The second-order polynomial equation used to predict the response surface Y is given by

$$Y = b_0 + \sum b_{1i}x_i + \sum b_{2i}x_i^2 + \sum b_{3ij}x_i x_j \quad (3)$$

and for four factors, the selected polynomial could be expressed equally

$$\text{TSFL} = b_0 + b_1(N) + b_2(S) + b_3(D) + b_4(Q) + b_{12}(NS) + b_{13}(ND) + b_{14}(NQ) + b_{23}(SD) + b_{24}(SQ) + b_{34}(DQ) + b_{11}(N^2) + b_{22}(S^2) + b_{33}(D^2) + b_{44}(Q^2) \quad (4)$$

Where  $b_0$  is the average of the responses and  $b_1, b_2, b_3, \dots, b_{44}$  are regression co-efficients [17] that depend on respective linear, interaction, and squared terms of factors. The value of co-efficient was calculated using Design Expert software. The significance of each co-efficient was calculated by student's t-test and p-values, which are presented in Table 7. Values of "Prob >F" less than 0.05 indicate that model terms are significant. In this case N, S, D, Q, ND, SD, DQ, N<sup>2</sup>, S<sup>2</sup>, and Q<sup>2</sup> are significant model terms. Values greater than 0.1 model terms are insignificant. The final empirical relationship was developed using only these co-efficients, and the developed final empirical relationship is given below

$$\text{TSFL} = \{ +12.18 + 0.28N + 0.37S + 0.49D + 0.34Q - 6.250E-003NS - 0.050ND - 0.037NQ - 0.069$$

$$SD - 0.13SQ + 0.040DQ - 0.87N^2 - 0.50S^2 - 0.046D^2 - 0.94Q^2 \} \text{ kN} \quad (5)$$

The adequacy of the model is tested by using Analysis of Variance (ANOVA). The test results of the ANOVA are given in Table 8. The desired confidence level was 95%. The relationship may be considered to be adequate. If that the calculated value of the F-ratio of the developed relationship does not exceed the tabulated value of F-ratio for a desired level of confidence, and the model is found to be adequate. The model F value of 95.87 implies that the model is adequate. There is only a 0.01% chance that a model F value this large could occur due to noise. The lack of fit F value of 1.67 implies that the lack of fit is insignificant. There is only 29.67% chance that a lack of fit F value this large could occur due to interference. Each predicted value matches with the experimental value as well shown in Fig. 8. The Fisher's F-test with a very low probability value demonstrates a very high significance of the regression model.

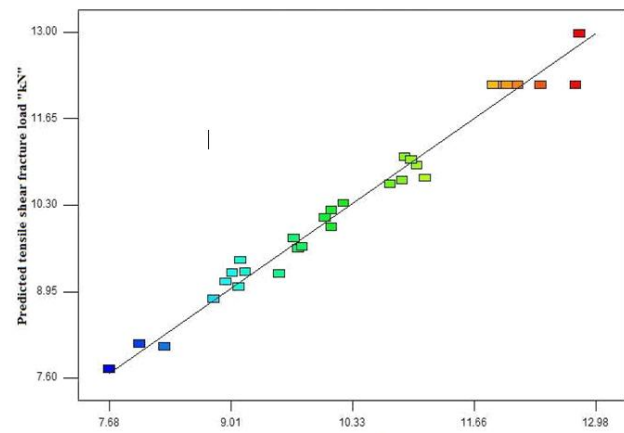


Fig.8. Correlation graph

The goodness of fit of the model is fitted by the determination coefficient ( $R^2$ ). The coefficient of determination was calculated to be 0.9889 in response, which implies that 98.8% of the experimental values confirm the compatibility with data as predicted by the model. The  $R^2$  value should always be between 0 to 1. If a model is statistically good, the  $R^2$  value should be close to 1.0. Then adjusted  $R^2$  value reconstructs the expression with the significant terms. The value of adj.  $R^2 = 0.9786$  is also high and indicates the high significance of the model. The pred.  $R^2$  value is 0.9473, which means that the model could explain 94% of the variability in prediction. This is in reasonable agreement with the Adj.  $R^2$  of 0.9786. The value of the coefficient of variation is as low as 2.84, which indicates that the deviation between experimental and predicted values is low. Adequate measures of the signal to noise ratio, a ratio greater than 4 is desirable. During this investigation, the ratio is 29.721, which indicates an adequate signal. This model can be used to navigate the design space. Fig. 7 shows the correlation graph of predicted and actual TSFL; it could indicate that the deviation between the actual and predicted TSFL is low.



Table 7. Calculated values of coefficients

Coefficient	FactorEstimate
Intercept	12.18
N	0.28
S	0.37
D	0.49
Q	0.34
NS	0.006
ND	0.05
NQ	0.037
SD	0.069
SQ	0.13
DQ	0.40
$N^2$	0.87
$S^2$	0.50
$D^2$	0.046
$Q^2$	0.94

#### 4. OPTIMIZING FSLW PARAMETERS

The response surface methodology (RSM) was used to optimize the friction stir lap welding (FSLW) parameters considered in this investigation. RSM is collection of mathematical and statistical technique that are useful for designing a lot of experiments, producing a mathematical model, examining for the optimal combination of input parameters and pressing out the value in graphically [18, 19]. Figure 9 illustrates the perturbation plot for the response TSFL of FSLW joints. This plot provides a silhouette view of the response and shows the change of TSFL, when each FSLW parameter moves from the reference point, with all other parameters held constant as the reference value. Design of the experiment sets the reference point default in the middle of the design space.

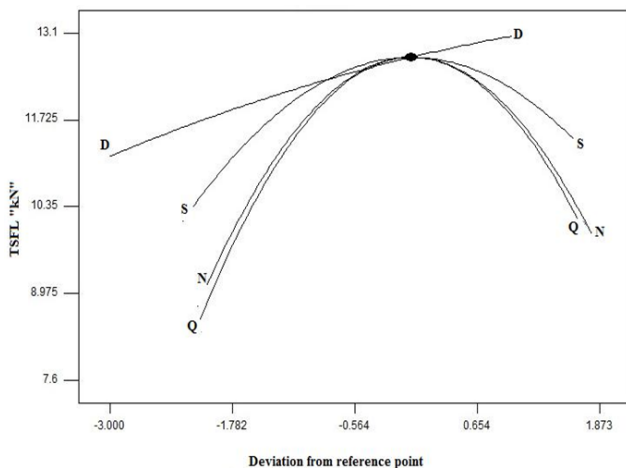


Fig.9. Perturbation graph

To obtain the influencing nature and optimized condition of the process on TSFL, the surface and contour plots which are indications of possible independence of factors have been built up for the proposed empirical relation considering two parameters in the halfway tier, and two parameters in the X-axis and Y-axis as shown in Fig.10. These response contours can help in the prediction of the response (TSFL) of any zone in the design domain [20]. The apex of the response plot shows the maximum achievable TSFL. A contour plot is produced to display the region of the optimum factor setting visually for second order responses, such a plot can be more complex compared to the simple series of parallel lines that can occur with first order models. Once the stationary point is found, it is usually necessary to characterize the response surface in the immediate vicinity of the point. Characterization involves identifying whether the stationary point is a minimum response or maximum response or a saddle point to classify this; it is more straightforward to analyze it through a contour plot. The contour plot plays a very important role in the study of a response surface. It is clear from that when the TSFL increases with increasing tool rotational speed, tool tilt angle and welding speed to a certain value and then decreases. It is likewise noted that the initial increase of the shoulder diameter increases the TSFL to a certain value and further addition of shoulder diameter makes a TSFL remain constant.

By analyzing the response surface and contour plots as shown in Figure 10 (a-f), the maximum achievable TSFL value is found to be 12.712 kN. The corresponding parameters that yield this maximum value are tool rotational speed of 912.7 rpm, welding speed of 112.76 mm/min, tool shoulder of 12.12 mm and tool tilt angle of 2.03. The higher F ratio value implies that the respective levels are more significant. From the F ratio value, it can be concluded that the tool tilt angle is contributing the major factor to exploit TSFL, followed by tool shoulder, welding speed and tool rotational speed for the range considered in this investigation. Figure 10 (a-f) indicates the response surface and contour plots representing the interaction effect of any two input parameters on the TSFL.

To validate the developed relationship, three confirmation experiments were carried out with the welding process parameters chosen randomly from the feasible working range (Table 4). The actual response was calculated as the average of three measured results. Table 9 and Table 10 summarize the experimental values, predicted values and the variation. The validation results revealed that the relationship developed is quite accurate as the variation in prediction is  $\pm 5\%$ .

Table 8. ANOVA test results

Source	Sum of squares (SS)	Degree of Freedom (df)	Mean square (MS)	F value	P-Value Prob>F	Model Significant or Not
Model	38.88	14	2.78	95.87	<0.0001	significant
N	0.96	1	0.96	33.27	<0.0001	
S	1.17	1	1.17	40.55	<0.0001	
D	1.62	1	1.62	55.82	<0.0001	
Q	2.04	1	2.04	70.27	<0.0001	
NS	0.061	1	0.06	12.11	0.1907	
ND	0.35	1	0.35	12.12	0.0051	
NQ	0.064	1	0.064	2.20	0.1826	
SD	0.41	1	0.41	14.25	0.0029	
SQ	0.089	1	0.089	3.05	0.1205	
DQ	0.57	1	0.57	19.81	0.0008	
N <sup>2</sup>	14.36	1	14.36	495.77	<0.0001	
S <sup>2</sup>	10.50	1	10.50	362.34	<0.0001	
D <sup>2</sup>	0.71	1	0.71	24.58	0.0006	
Q <sup>2</sup>	15.37	1	15.37	530.62	<0.0001	
Residual	0.43	1	0.029			
Lack of fit	0.33	10	0.033	1.67	0.4978	Not Significant
Pure Error	0.10	5	0.02			
Cor Total	39.32	29				
Std.Dev	0.17		R <sup>2</sup>	0.9889		
Mean	6.00		Adj R <sup>2</sup>	0.9786		
C.V%	2.84		Pred.R <sup>2</sup>	0.9473		




Table 9. Validation test results for the developed empirical relationship

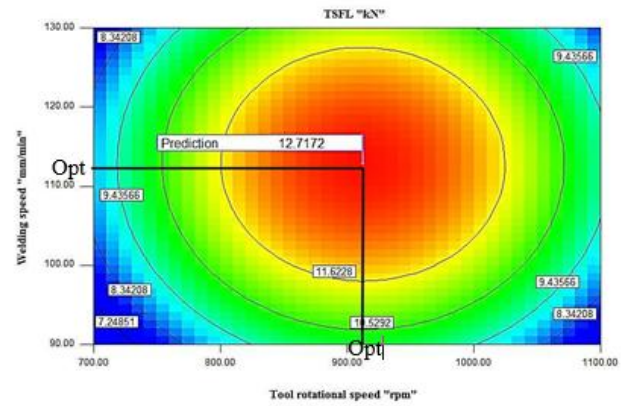
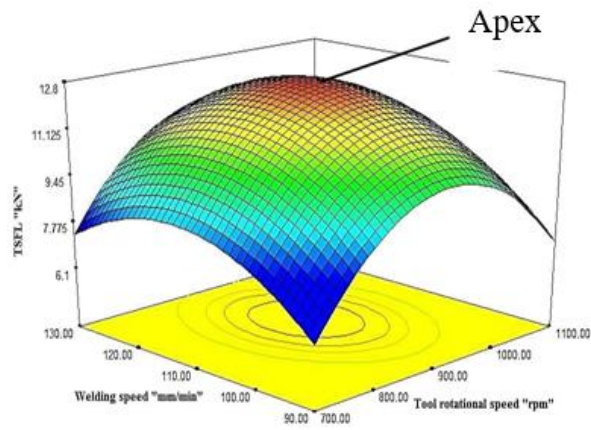
Sl. No	Tool rotational speed (rpm)	Welding speed (mm/min)	Tool shoulder diameter (mm)	Tool tilt angle (°)	Actual TSFL (kN)	Predicted TSFL (kN)	% Error
01	920	115	12	2	11.85	10.15	0.14
02	900	110	14	2.5	12.12	11.02	0.09
03	890	100	10	2.5	12.41	12.45	0.03

Table 10. Validation test results for optimization procedure

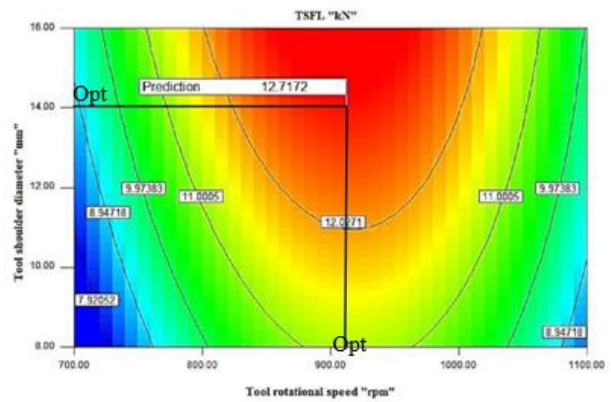
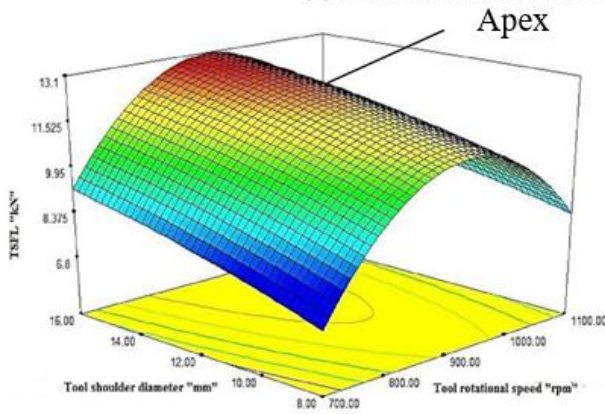
Sl. No	Tool rotational speed (rpm)	Welding speed (mm/min)	Tool shoulder diameter (mm)	Tool tilt angle ( $^{\circ}$ )	Actual TSFL (kN)	Predicted TSFL (kN)	% Error
01	913	112	12	2	12.71	11.81	0.07
02	915	112	14	2	12.72	12.37	0.02
03	908	112	14	2	12.71	12.88	0.01

Table 11. Cross-sectional macrograph of FSLW joints

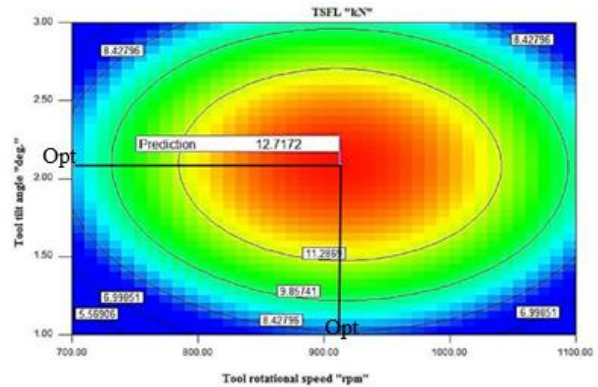
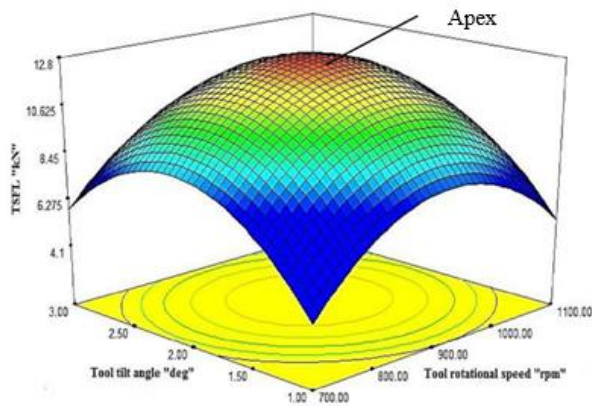
Joint No	Macrograph	TSFL (kN)
01		8.28
09		9.09
25		12.76



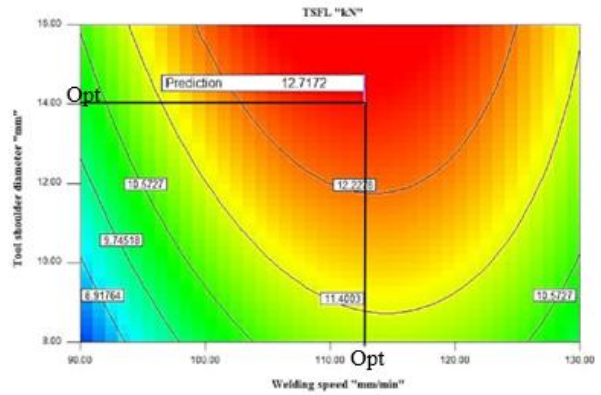
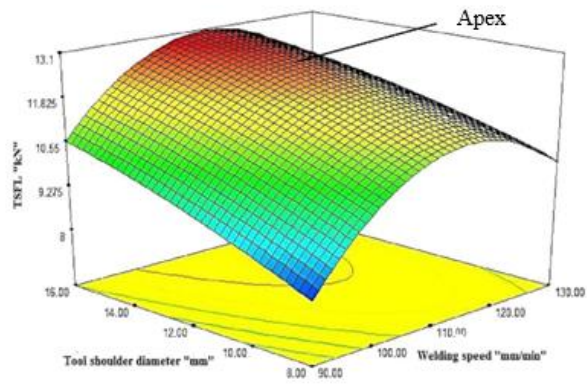
(a) Interaction effect of tool rotational speed and welding speed



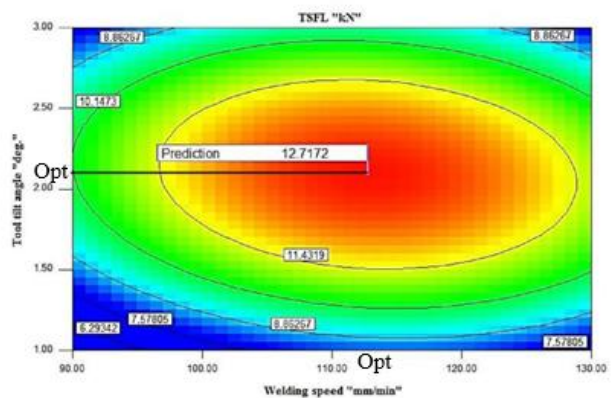
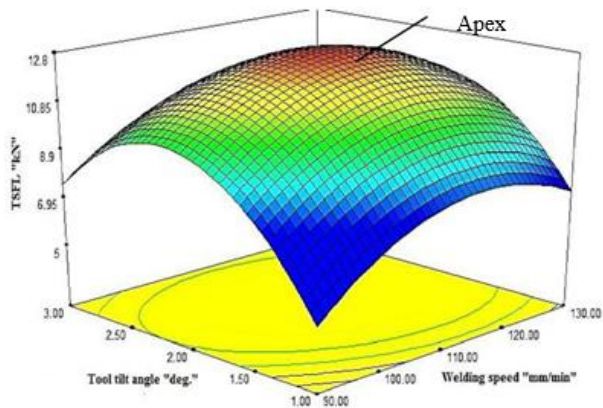
(b) Interaction effect of tool rotational speed and tool shoulder diameter



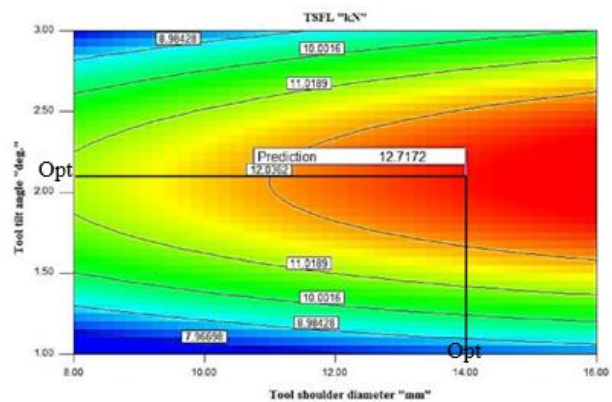
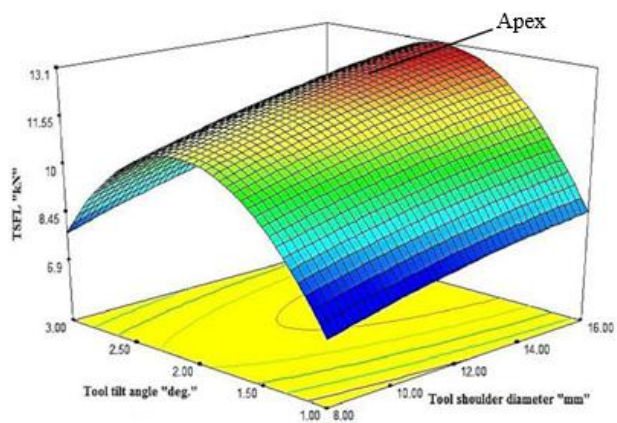
(c) Interaction effect of tool rotational speed and tool tilt angle



(d) Interaction effect of tool shoulder diameter and welding speed

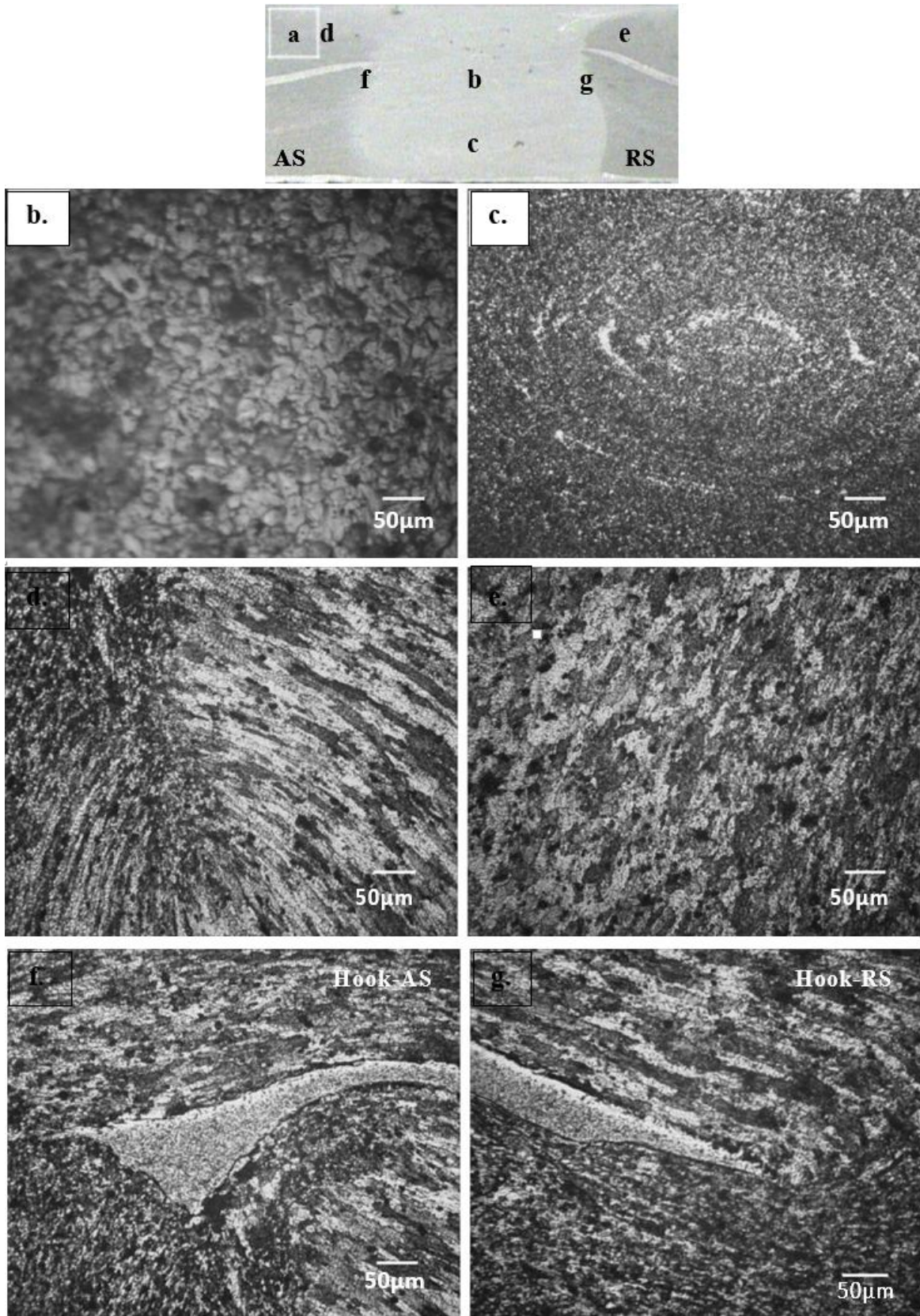


(e) Interaction effect of tool tilt angle and welding speed



(f) Interaction effect of tool shoulder diameter and tool tilt angle

**Fig. 10. Response surface graphs and contour plots**



**Fig. 11. Optical micrograph of the FSLW joint (Joint No 25)**

## 5. MICROGRAPH OF FSLW JOINT

The macrographs of friction stir lap welded joint made using different parameters are shown in Table 11. The FSLW joint is conventionally divided into four regions, stir zone (SZ), thermo-mechanical heat affected zone (TMAZ), heat affected zone (HAZ) and base metal (BM). The size of the SZ is closely related to the pin geometry. The formation of SZ is due to the combined effect of thermal and mechanical stresses caused by stirring action of the non-consumable tool and axial force. The micrographs of the various region of the optimized FSLW joint (Joint no 25) are shown in Figure 11. The SZ (Fig. 11b) shows fine and recrystallized equiaxed grains produced by severe plastic deformation. Fewer second phase strengthening precipitates of uniformly distributed Al<sub>2</sub>Cu are observed in SZ, towards the weld bottom distinct onion ring pattern is also seen (Fig. 11c). The micrographs of TMAZ are shown in Figure 11d and Figure 11e. The TMAZ in FSLW joint showed severely deformed non - recrystallized grains, but there is no significant grain coarsening in the HAZ. Within the region covered by the tool shoulder two distinct bond regions are observed in lap weld. They are: the partially bonded region and fully bonded region. The partially bonded region has been described by few investigators as original joint line with severe plastic deformation (O)lWSPD [21], bond line [22] and interface [17]. The upper and lower sheets closely mate with each other. They are separated by a thin layer beginning somewhere near the tool shoulder mark on either side of the weld and extend inwards, ending either at the TMAZ/SZ interface or SZ. In this weld the partially bonded region was observed to extend into TMAZ/SZ (Fig. 11f and Fig.11g). The second one is fully bonded region, the region within stir zone, where the upper and lower sheet get metallurgically bonded with each other with no discernible original interface line in the weld. The width of the fully bonded region is an important consideration in lap joint. When the thread rotates in the favorable direction it can result in such a strong downward metal flow [23-25]. The reason for lower lap shear strength of AA2014-T6 aluminum alloy is due to different relative speeds of plastic material on advancing side and on retreating side which results in different microstructure [26]. It is found on the advancing side; the speed gradient is greater than the retreating side. Microstructure changes rapidly and there is lack of necessary transition. Hook is an important consideration in the friction stir lap welding, it could indicate the flow of material around the rotating pin. In this investigation, both the hooks bent toward the SZ bottom.

## 6. CONCLUSIONS

1. An empirical relationship has been developed and to predict the tensile shear fracture load of friction stir lap welded AA2014-T6 aluminum alloy joints with 95% confidence level, incorporating predominant parameters.
2. A maximum tensile shear fracture load of 12.76 kN could be achieved under the rotational speed of 900 rpm,

welding speed of 110 mm/min, tool shoulder diameter of 12 mm, and tilt angle of 1.5°

3. Of the four process parameters investigated, the tool tilt angle (based on F value) was found to have the greater influence on tensile shear fracture load followed by tool shoulder diameter, welding speed, and rotational speed.

## ACKNOWLEDGEMENT

The authors wish to thank Aeronautical Development Agency (ADA), Bangalore, for the financial support to carry out this investigation through a R&D project no: FSED 83.07.03.

## REFERENCES

- [1] **Thomas W. M., Nicholas E. D., Needam J. C., Murch M. G., Templesmith P., Dawes C. J.** GB Patent application No: 9125978.8, December 1191 and US Patent No. 5460317, October 1995.
- [2] **Irving B.**, Why aren't airplanes welded? *Welding Journal* 76(1) (1997) 31-41.
- [3] MIL-HDBK-5H, *Metallic materials and elements for aerospace vehicle structure* (1998) 8-27, 37, 108, 148.
- [4] **Fadaeifard F., Matori K. A., Toozandehjani M.**, Influence of rotational speed on mechanical properties of friction stir lap welded 6061-T6 Al alloy, *Trans. Nonferrous Met. Soc. China* 24 (2014) 1004-1011.
- [5] **Urso G. D., Giardini C.**, The influence of process parameters and tool geometry on mechanical properties of friction stir welded aluminum lap joints, *Int. J. Mater. Form.* 3 (1) (2010) 1011-1014.
- [6] **Yazdani S., Chen Z. W.**, Effect of friction stir lap welding conditions on joint strength of aluminum alloy 6060, *Materials science and Engineering* 4 (2009) 012021
- [7] **Soundarajan V., Yarrapareddy E., Kovacevic R.**, Investigation of the friction stir lap welding of aluminum alloys AA5182 and AA6022, *Journal of Materials Engineering Performance* 16 (2007) 477-484.
- [8] **Kimpong K., Watanabe T.**, Effect of welding process parameters on mechanical property of FSW lap joint between aluminum alloy and steel, *Materials Transactions*, 46 (10) (2005) 2211-2217.
- [9] **Cen Z.W, Yazdani S.**, Friction stir lap welding: material flow, Joint structure and strength, *Jour. Of Achievements in Materials and Manufacturing Engineering* 55 (2012) 629-637
- [10] **Babu S., Janakiram G. D., Venkatakrishnan P. V., Madusudhana Reddy G., Prasad Rao K.**, Microstructure and mechanical properties of friction stir lap welded aluminum alloy AA2014, *J. Mater. Sci. Technol.*, 28 (5) (2012) 414-426.
- [11] **Galvao I., Verdera D., Gesto D., Loureiro A., Rodrigues D. M.**, Influence of aluminum alloy type on dissimilar friction stir lap welding of aluminum to copper, *Journal of Material Processing Technology* 213 (2013) 1920-1928.
- [12] **Buffa G., Campanile G., Fratini L., Prisco A.**, Friction stir lap joints: Influence of process parameters on the metallurgical and mechanical properties, *Mater. Science and Engineering A*, 519 (2009) 19-26.
- [13] **Cen Y. C., Nakata K.**, Friction stir lap joining aluminum and magnesium alloys, *Scripta materialia* 58 (2008) 433-436.

- [14] **Salari E., Khodabandeh A.**, Friction stir lap welding of 5456 aluminum alloy with different sheet thickness: process optimization and microstructure evaluation, *The Int. Jou of Adv Manu. Tech.*, 82 (2016) 39-48
- [15] **Shirazi H., Kheirandish Sh., Safarkhanian M. A.**, Effect of process parameters on the macrostructure and defect formation in friction stir lap welding of AA5456 aluminum alloy, *Jour. Of Measurement*, 76 (2015) 62-69.
- [16] **Zhengwei Li, Yumei Yue, Shude Ji, Peng Chai, Zhenlu Zhou**, Joint features and mechanical properties of friction stir lap welded alclad 2024 aluminum alloy assisted by external stationary shoulder, *Material & Design*, 90 (2016) 238-247.
- [17] **Jamshidi H., Serajzadeh S., Kokabi A.**, Theoretical and experimental investigation in to friction stir welding of AA5086, *Int. j. Adv. Manu. tech.* 52 (2011) 531-544.
- [18] **Khuri A. I., Cornel I. J.**, *Response surfaces; design and analysis.* Marcel Dekker, New York (1996)
- [19] **Gunaraj V., Murugan N.**, Application of response surface methodology for predicting weld bead quality in submerged arc welding of pipes. *J Mater Process Technol*, 88 (1999) 266-275.
- [20] **Tien C.L., Lin S.W.**, Optimization of process parameters of titanium dioxide films by response Surface Methodology. *Opt Common* 266 (2006) 574-581.
- [21] **Cao X. Jahazi M.**, Effect of tool rotational speed and probe length on lap joint quality of friction stir welded magnesium alloy, *Materials & Design*, 32 (2011) 1-11.
- [22] **Ghosh M., Kumar K., Mishra R.S.**, *Mater. Sci. Eng. A* (2011) 528, 8111.
- [23] Mishra R. S., Ma Z. Y., Friction stir welding and processing, *Mater. Sci. Eng. R* 50 (2005) 1-78.
- [24] **Nandan R., Debroy T., Bhadesahia H. K. D. H.**, Recent advances in friction-stir welding - Process, weldment structure and properties, *Prog. Mater. Sci.* 53 (2008) 980.
- [25] **Buffa G., Hua J., Shivapuri R., Fratni I.**, A continuum based fem model for friction stir welding—model development, *Mater. Sci. Eng A*, (2006) 419, 381.
- [26] **Zhao Y., Lin S., Wu L., Qu F.**, The influence of pin geometry on bonding and mechanical properties in friction stir weld 2014 Al alloy, *Mater. letter* 59(23) (2005) 2948-2952.